EFFECT OF SKEW ANGLE ON LIVE LOAD DISTRIBUTION OF SKEW COMPOSITE GIRDER BRIDGE

Md Basir ZISAN*[1], M. Z. MOUSUMI[2] and Md Naimul HAQUE[3]

[1]*Faculty, Department of Civil Engineering, CUET, Bangladesh, e-mail: basirzisan@gmail.com*
[2]*Student, Department of Civil and Environmental Engineering, SUST, Bangladesh, e-mail: mzmzisan@gmail.com*
[3]*Faculty, Department of Civil Engineering, CUET, Bangladesh, e-mail: naimulce@gmail.com*

ABSTRACT

The objectives of this paper is to evaluate the lateral live load distribution factor (LDF) of a composite curved-skew bridge and also compares the obtain values with AASHTO LFRD code value. The LDFs were investigated for the transverse vehicle positions on bridge deck and skew bridge support conditions. A numerical transient dynamic analysis was performed using a three-dimensional (3-D) finite element (FE) model of bridge-vehicle-interaction (BVI) system. The BVI model consists of a space bridge-vehicle system and a contact model. The entire modeling and analysis were performed using ANSYS. Inertia and horizontal force, friction and road roughness were taken into account for the reality of the problem. The analysis results show that the AASHTO LRFD code overestimated the LDF value. The vehicle transverse position on the bridge deck and skew angle has substantial influence of LDF and for exterior girder LDF differs significantly with interior girder.

Keywords: *ANSYS, skewed bridge, bridge vehicle interaction, transient dynamic analysis, load distribution factor*

1. INTRODUCTION

A bridge is defined as a skew bridge when normal of the bridge centerline makes an angle with the support centerline. The skew bridge differs from non-skew bridge for the load transfer mechanism between two support ends. In a skew bridge, the load path changes from the bridge centerline to the diagonal direction which significantly increase the torsion (Nouri & Ahmadi, 2012). The computation of dynamic responses for such bridges under dynamic vehicular load is a complex procedure. The moment demand of a particular girder depends on the position of vehicles on the bridge, load magnitude and the bridge geometry. The design moment depends on the number of girder, girder spacing, girder stiffness, diaphragm, deck thickness (Barr et al., 2001). To simplify the design process AASHTO Standard Specification (AASHTO, 1996) and AASHTO Load and Resistance Factor Design (AASHTO LRFD, 1998) proposed the following formula presented by equation (1) and equation (2), respectively which are applied to a concrete bridge supported by steel girders.

$$LDF = S/5.5 \quad \text{(US customary unit)} \qquad (1)$$

$$LDF = 0.06 + \left(\frac{S}{4300}\right)^{0.4} * \left(\frac{S}{L}\right)^{0.3} * \left(\frac{K_g}{Lt_s^3}\right)^{0.1} \quad \text{(SI unit)} \qquad (2)$$

where, S is girder spacing, L is bridge span length, $K_g = n(I+Ae^2)$ is girder longitudinal stiffness t_s is bridge deck thickness, A is girder area, e is the eccentricity between centroids of girder and concrete deck and n is modular ratio. The distribution factor calculated by the above mentioned formula, multiply by the moment on a single girder caused by the single line of wheel load gives the girder design moment. These procedures are only applicable for simply supported non-skew and straight bridges. Compare to the AASHTO LRFD, the AASHTO Standard equation tends to give unconservative lateral load distribution (LDF) when bridge span length and girder spacing are relatively small, and gives overly conservative LDF when bridge span length and girder spacing are relatively large. The AASHTO Standard procedure is simple and gives erroneous LDF while the AASHTO LRFD gives more accurate results but cumbersome in practice. The FE model used for development of AASHTO LRFD LDF equations did not considered the important bridge features like diaphragm, cross bracing, bridge curvature and skews. The parametric study (Eamon & Nowak, 2004) indicates bridge secondary elements have a significant effect on the LDF. Consequently, the AASHTO LRFD equation often provides overly conservative results. Also AASHTO Standard Specification does not distinguish the exterior and interior

girder, nor do they consider the bridge skewness, vehicle configuration and important bridge and vehicle features.

The purpose of paper is to evaluate the use of commercial FE code, ANSYS for the computation of LDF of a composite curve-skewed bridge supported by multi steel I-girder and employ this analysis to investigate the effect of the skew angle on LDF of curved-skew deck under moving vehicle. For this purpose, a versatile and computationally efficient bridge-vehicle-interaction model is developed using space bridge and vehicle structure modeled by ANSYS program. The vehicle is modeled as three-axle mass-spring-damper system. The analysis considered the approach road, inertia force, centrifugal force, deck friction and the vehicle model include the effect of pitching, rolling, bouncing and separation between tires and bridge surface.

2. FINITE ELEMENT MODELING

2.1 Bridge Modeling

The finite element (FE) model of the bridge consists of five main I-girders, each of 2.8 m deep and equally spaced by 2.1 m, which were bonded with overlaying reinforced concrete slab and tied together with 10 equally spaced diaphragms. Table 1 describes the basic geometric properties of the original bridge which has a radius of 1000 m and skew angle 0° as shown in Fig. 1a and Fig. 1b. Table 2 indicates the calculated girder properties. Fig. 1c shows the FE model for the bridge with right-angle diaphragm modeled by ANSYS in which, the skew angle varies from 0° to 45° and 1000 m radius. The bridge was modeled by using 8-noded SOLID45 hexagonal elements for concrete deck and 4-noded quadrilateral SHELL63 element for all steel members. SOLID 45 and SHELL 63 elements has 3 & 6 DOFs in each node, respectively, and both elements have large deflection capability to perform nonlinear analysis (ANSYS Inc., 2012). Cylindrical coordinate system having origin at the

Table 1: Basic geometric properties of Kita-go bridge (Zisan et al., 2015)

Span length (mm)	49913			
Deck width*thickness (mm)	11000*20			
Web of main girder (mm)	WEB 2800*10			
Flange of main girder (mm)	FLGG1	FLGG2	FLGG 3&4	FLGG5
	540*25	350*16	370*14	510*25
Vertical Stiffener of main girder (mm)	145*12			
Horizontal Stiffener of main girder (mm)	115*11			
Flange and Web of Intermediate Diaphragm (mm)	IFLG 100*8 and IWEB 200*8			
Vertical Stiffener of Intermediate Diaphragm (mm)	145*12			
Flange and Web of End Diaphragm (mm)	EFLG 250*10 and EWEB 2400*9			
Vertical Stiffener of End Diaphragm (mm)	145*22			
Flange and Web of Lateral Bracing	LWEB 150*10 and LFLG 150*12			
Skew angle	0°, 15°, 30° and 45°			
Radius (m)	1000			

Table 2: Calculated Bridge Steel Girder properties

Girder	Area ($x10^4$ mm^2)	Eccentricity from slab midpoint e (mm)	Moment of Inertia I ($x10^{10}$ mm^4	Torsional Inertia J ($x10^{10}$ mm^4	Longitudinal Stiffness $K_g = n(I+Ae^2)$ ($x10^{10}$ mm^4)
1	5.45	1300	6.93	7.00	129.1
2	3.89	1300	3.94	3.95	84.07
3 &4	3.81	1300	3.79	3.80	81.77
5	5.30	1300	6.64	6.70	124.8

Table 3: Boundary conditions

Support condition	u_1	u_2	u_3	θ_1	θ_2	θ_3
Roller	Fix	Free	Fix	Free	Free	Free
Hinged	Fix	Fix	Fix	Free	Free	Free

u_1, u_2, u_3 are translations in R, θ, Z directions
θ_1, θ_2, θ_3 are rotations in R, θ, Z directions

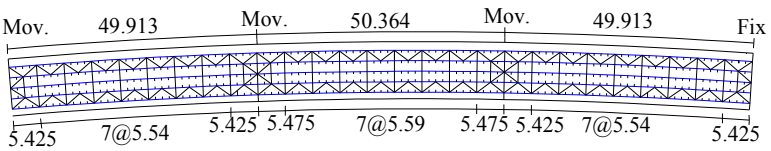

(1a) Plan View

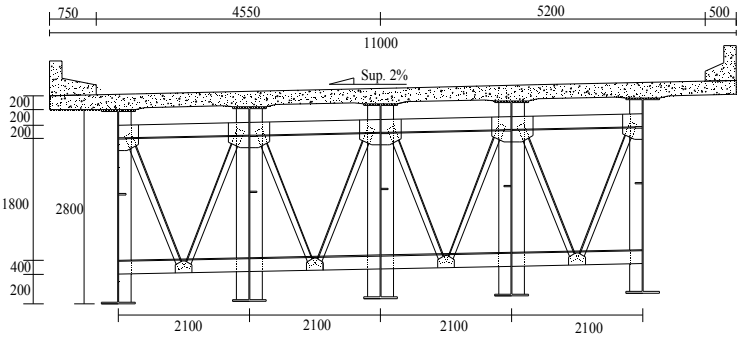

(1b) Cross section

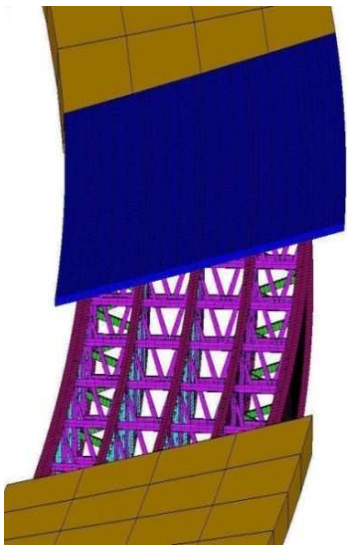

(1c) FE model of bridge with 30^0 skew angle

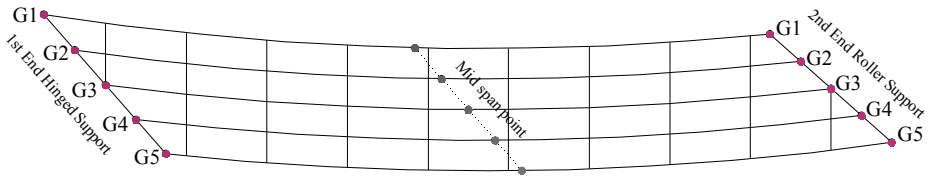

Figure 1: Geometric properties of Kita-gothe bridgee and FE models of bridge

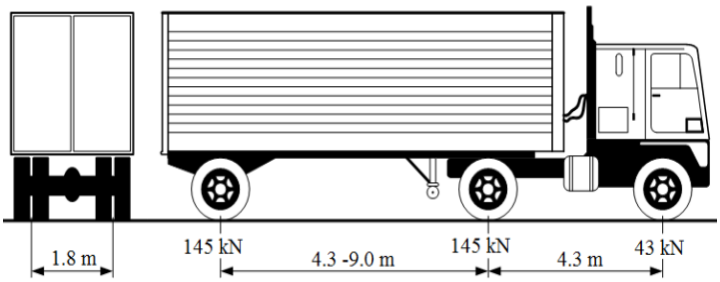

(2a) AASHTO HS20-44 truck

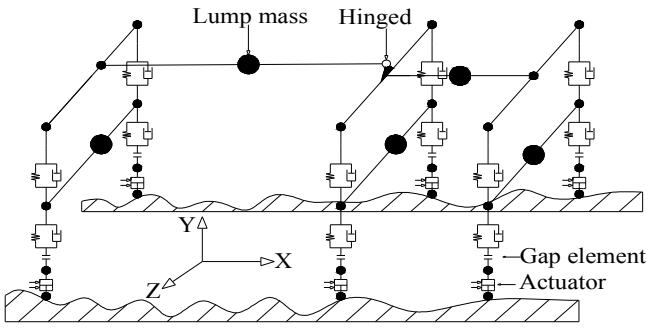

(2b) FE model of HS20-44 truck

Figure 2: AASHTO HS20-44 design vehicle

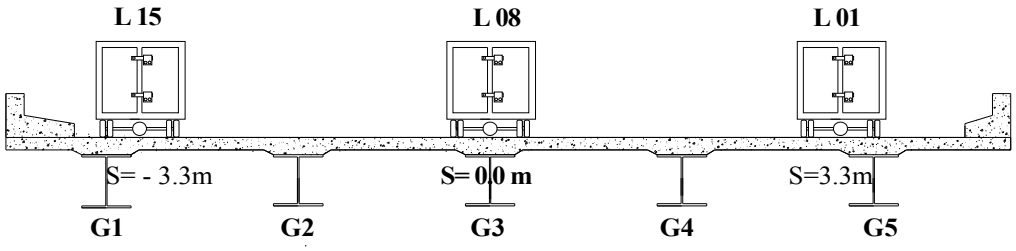

Figure 3: Transverse vehicle positions

Table 4: Stiffness coefficient of HS20-44 Design truck (Wang & Huang, 1992)

	Front axle (kN/cm)	Drive axle (kN/cm)	Semi-trailer axle (kN/cm)
Tire	8.75	35.03	35.07
Suspension spring	2.43	19.03	16.69

center of the bridge curvature was used to define all geometric properties of FE models. Simply supported boundary conditions, roller and hinge supports were used at the bottom flange node of each girder ends. Table 3 shows the boundary conditions for the bridge end. The moduli of elasticity and the mass density of steel and concrete were taken as 210 GPa & 7850 kg/m^3 and 28.57 GPa & 2500 kg/m^3, respectively. The Poisson ratios of steel and concrete were assumed 0.3 and 0.2, respectively. The skew angles 0°, 15°, 30° and 45° were taken to illustrate the effect of the skew angle. All displacement components for the bridge were computed at the middle of the girder as shown in Fig. 1d and the girder reactions were calculated for the 1st end bearing.

2.2 Vehicle Modeling

The FE model of HS20-44 design truck, specified by AASHTO, consists of six wheels and three-axle tractor-trailer as shown in Fig. 2a. A 3-D nonlinear FE model of the HS20-44 truck was developed using ANSYS, which consists of five lump-masses representing tractor, semi-trailer and three axle sets as shown in Fig. 2b. All masses were connected with rigid beam and supported by linear spring-dampers forming the vehicle body were modeled using MASS21 and BEAM4 elements, respectively. The upper and lower spring damper representing suspension of the vehicle body and tires were modeled by COMBIN40 element consists of parallel spring-slider and damper coupled with a gap in the series. The separation between tire and road was integrated using gap element at the lower spring-damper. The tire stiffness and spring suspension values were found from (Wang & Huang, 1992) as shown in Table 4. To simulate the road roughness, an actuator modeled by LINK11 element was connected with gap element. The suspension force consists of linear elastic spring force and constant interleaf friction force. Three vehicle positions named outside (L01), central (L08) and inside (L15) were considered as shown in Fig. 3.

Figure 4: Road roughness profile for wheel track

2.3 Road Roughness Modeling

The road surface roughness was assumed as a periodically modulated random process derived from Power Spectral Density (PSD) function (Dodds and Robson, 1973) expressed exponentially using Eq. (1).

$$S(n) = S(n_0)\left(\frac{n}{n_0}\right)^{-w} \quad (1)$$

where, $S(n)$ is PSD (m^2/cycle/m); n is wave number (cycle/m); $S(n_0)$ is roughness coefficient (m^2/cycle/m); n_0 is discontinuity frequency is 1/ (2π); Based on Motor Industry Research Association specification (Labarre et al., 1969), w is 2 (1.36 ~2.28) for principle road and roughness coefficient is $20*10^{-6}$ for good surface. For vehicle bouncing, pitching and rolling effect, different roughness profiles for both tracks as shown in Fig. 4 were derived from PSD and cross spectral density functions considering the road surface as a homogenous and isotropic random process using Eq. (2) and Eq. (3) (Awall, 2012).

$$y(x)=\sum_{i=1}^{N}\left(\sqrt{\Delta n_i S(n_i)}\ \cos\left(2\pi n_i x+\varphi_i\right)\right) \quad (2)$$

$$y_R(x) = \sum_{i=1}^{N}\left(\sqrt{\Delta n_i . S_x(n_i)}\ . \cos\left(2\pi n_i x+\varphi_i\right) + \sqrt{\Delta n_i (S(n_i)\ S_x(n_i))}\ . \cos(2\pi n_i x+\theta_i)\right) \quad (3)$$

Where, $S_x(n)$ is cross spectral density, Φ_i, θ_i is 1st and 2nd random phase angle, x is longitudinal distance, N is the number of sinusoidal components, *and* Δni is bandwidth.

2.4 Bridge Vehicle Interaction Modeling

BVI problems consist of two separate bridge and vehicle systems where contact point and contact force between vehicle tires and road surface changes from time to time. Here node to surface contact technology supported by ANSYS was used to model the interaction between the bridge and vehicle. ANSYS CONTA174 and TARGE170 elements were used to generate node to contact surface and target surface respectively. CONTA174 element supports large sliding, large deformation, Coulomb friction and provides better contact result16). In this study, an isotropic coulomb friction of value 0.18 was assumed in all cases (Samaan et al., 2007). This contact technology allows the contact node to slide over the target surface with friction, which dramatically adds non-linearity of the analysis.

3. TRANSIENT DYNAMIC ANALYSES

The transient dynamic analysis is a technique used to determine the dynamic response of a structure under the action of any general time-dependent loads. The basic equation of motion solved by a transient dynamic analysis is given in equation (4). The Rayleigh damping and lumped-mass were assumed and 1% critical damping was assumed for 1st and 2nd natural mode. Newmark's β and Newton-Raphson methods with transient option (ANSYS Inc., 2012) were used to calculate the structural response. The friction force between tires and pavement mainly depends on the types of pavement surface and tire characteristics. A frictional coefficient of value 0.18 was used in all cases. The vehicle was assumed to run at a constant speed 105 km/hr along different periphery and to obtain the initial conditions of the vehicle; it was subjected to run an approach road of 45 m length having surface roughness same as that of bridge deck before entering the bridge. In all cases, good surface roughness condition was considered. The LDF of the curved-skew bridge was invested for transverse vehicle position and skew support condition.

$$[M]\{\ddot{u}\} + [C]\{\dot{u}\} + [K]\{u\} = \{F(t)\} \quad (4)$$

where, [M] is mass matrix, [C] is damping matrix, [K] is stiffness matrix, $\{\dot{u}\}$is nodal velocity vector, $\{\ddot{u}\}$ is nodal acceleration vector, {u} is nodal displacement vector and {F(t)} is load vector.

4. LIVE LOAD DISTRIBUTION FACTOR (LDF)

To obtain the maximum girder moment, the AASHTO HS20-44 design trucks were first run along longitudinally over the bridge at a speed of 105 km/hr. In every analysis, the maximum response of each girder said bearing force and bending stress were first find out. The individual girder moment and the total bridge

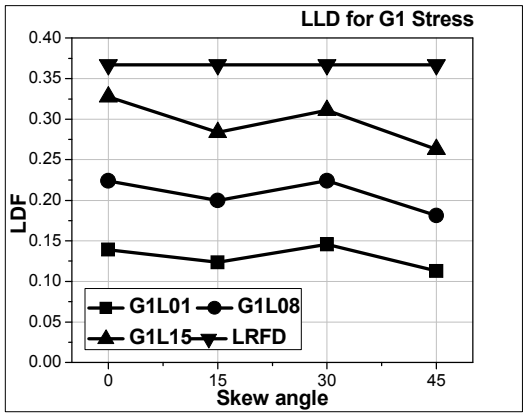

(5a)

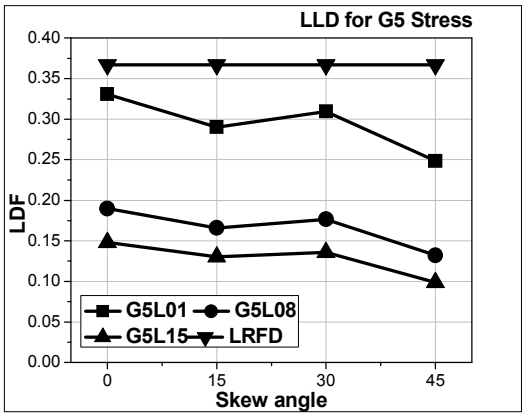

(5b)

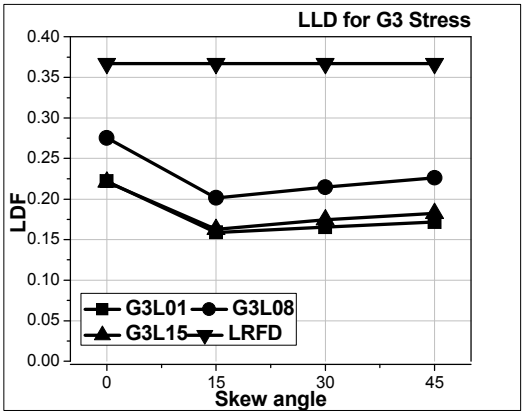

(5c)

Figure 5: Lateral Live Load Distribution for Bending Stress (5a, 5b, 5c)

response, i.e., summation of each girder response, for each transverse truck location was calculated. The largest girder moment for all locations was selected as the maximum girder moment (Zokaie, 2000). The live load distribution factors were then calculated by dividing the maximum girder response (bearing force, stress, deflection) by bridge response. The live-load distribution factors were also calculated using the methods given in the AASHTO LRFD Specifications (1998) as explained in equation (2) for comparison purposes.

4.1 Live Load Distribution Factor for Stress

Fig. 5 describes the live load distribution factor based on bending stress measured at the mid-span of each girder. It also shows that the AASHTO LRFD code overestimated the LDF both for exterior and interior middle girder. The LDF for both exterior girder (G1 and G5) decreases with skew angle while for interior middle girder (G3) LDF increase softly for skew angle more than 15°. The effect of skewness for exterior girder is dominant compared to interior middle girder because of the diagonal load transfer mechanism. The LDF for each girder differ significantly for the exterior vehicle position (L1 and L15) while minor fluctuations for the central vehicle position (L08).

4.2 Lateral Load Live Distributions for Reaction

Fig. 6 describes the effect of skew angle on live load distribution factors based on the girder reaction force for single lane loading condition. It shows the distribution factor for inside exterior girder (Fig. 6a) decrease and

outside exterior girder (Fig. 6b) increase for the increase of skew angle. The LDF factor for both exterior girder (G1 and G5) is significantly higher than the interior middle girder (G3). It found both for the exterior vehicle position (L01 and L15) the LDF for the girder differ significantly while for interior vehicle position the difference is quite small. In each case, the ASHTO LRFD (1998) code overestimated the live load distribution

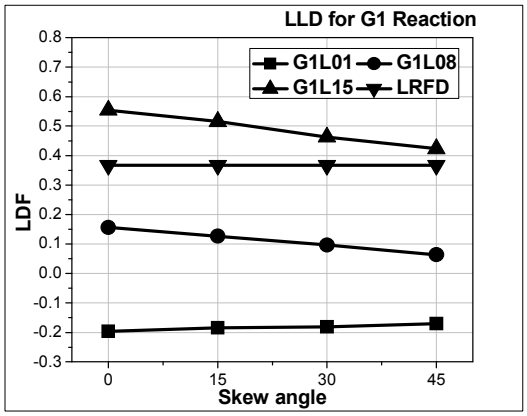

(6a)

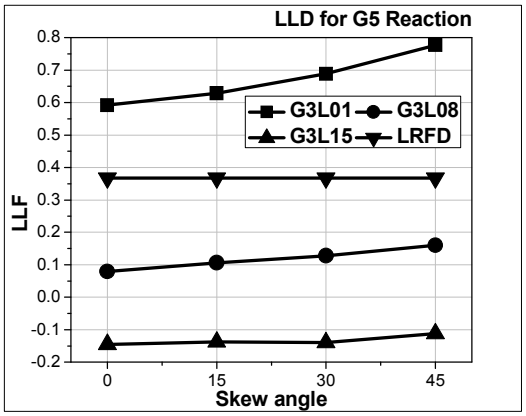

(6b)

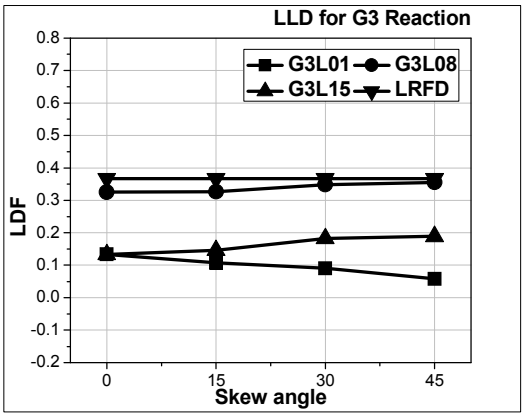

(6d)

Figure 6: Lateral Live Load Distribution for Support Reaction (6a, 6b, 6c)

factor and this overestimation is higher much higher than interior middle girder. The distribution factor for girder G1 and girder G5 shows completely reverse trend mainly for curvature of the bridge (Zhang et al., 2005). Also the transverse position of the vehicle on the bridge plays a vital role on the LDF. Fig. 6c shows, for the central position of the vehicle the LDF is quite independent of skew angle. But the LDF increase for inside position (L15) of the vehicle while it decreases for the outside position (L01) of the vehicle.

5. CONCLUSIONS

The effects of skew angle on lateral load distribution for a composite girder bridge were investigated under moving vehicle. For this purpose, a versatile and computationally efficient bridge-vehicle-interaction model developed using space bridge and vehicle structure modeled by ANSYS. The vehicle was modeled as three-axle mass-spring-damper system and the FE procedure considered the approach road, inertia force, centrifugal force, deck friction and bridge road surface roughness.

It is clear that the AASHTO LRFD overestimated the LDF for skew bridge. The bearing force LDF for exterior girder increases and decrease for interior girder with skew angle while for interior girder LDF changes softly. And the bending stress LDF decrease with skew angle both exterior girder and minor increase for interior girder

for skew angle more than 15°. The LDF for each girder differ significantly for exterior vehicle position while minor differences for central vehicle position.

REFERENCES

AASHTO Standard Specifications for Highway Bridges (1996). 16th Edition, *American Society of State Highway and Transportation Officials*, Washington, D.C.

AASHTO LRFD Standard Specifications for Highway Bridges (1998). 2nd Edition, *American Society of State Highway and Transportation Officials,* Washington, D.C.

ANSYS Inc. (2012). Release 13.0 *Documentation*, Theory References.

Awall, M. R., (2012). Dynamic behavior f horizontally curved twin I-girder bridge under moving vehicle, *PhD Thesis*, Hokkaido University.

Barr P. J., Eberhard, M. O. & Stanton J. F. (2001). Live-load distribution factors in prestressed concrete girder bridges, *Journal of Bridge Engineering*, Vol. 6 (5), pp. 298-306.

Dodds C. J. & Robson J. D. (1973). The description of road surface roughness, *Journal of Sound and Vibration*, Vol. 31(2), pp. 175-183.

Eamon, C.D. & Nowak A.S. (2004). Effect of Secondary Elements on Bridge Structural System Reliability Considering Moment Capacity, *Structural Safety*, Vol. 26, pp. 29-47.

Labarre, R. P., Forbes, R. T. & Andrew, S., (1969). The measurement and analysis of road surface roughness, *Motor Industry Research Association Report No.* 1970/5.

Nouri, G. & Ahmadi, Z. (2012). Influence of Skew Angle on Continuous Composite Girder Bridge. *Journal of Bridge Engineering,* Vol. 17(4), pp. 617–623.

Samaan M., Kennedy J. B. & Sennah K. (2007). Impact factors for curve continuous composite multiple-box girder bridges, *Journal of Bridge Engineering*, ASCE, Vol. 12(1), pp. 80-88.

Wang TL and Huang D (1992). Computer Modeling Analysis in Bridge Evaluation," *Final report – Highway Planning and Research Program*, Miami, Florida.

Zhang, H., Huang, D. & Wang, T. L. (2005). Lateral Load Distribution in Curved Steel I-Girder Bridges, *Journal of Bridge Engineering*, Vol. 10(3), pp. 281-290.

ZISAN M. B., HAYASHIKAWA T., MATSUMOTO T. & HE X. (2015). Dynamic response and distortion-stress in curved multi-girder bridges subjected to high-speed moving vehicles, *Journal of Structural Engineering, JSCE,* Vol.61A, pp. 119-130

Zokaie, T. (2000). AASHTO-LRFD live load distribution specifications. *Journal of Bridge Engineering*, Vol. 5(2), pp. 131–138.